REINFORCED MECHANICAL PROPERTIES OF FUNCTIONALIZED SILICA AND EGGSHELL FILLED GUAYULE NATURAL RUBBER COMPOSITES

XIANJIE REN,[1] YANG GENG,[2] ALFRED B. O. SOBOYEJO,[2] KATRINA CORNISH[3,*]

[1]DEPARTMENT OF FOOD, AGRICULTURAL AND BIOLOGICAL ENGINEERING, OHIO AGRICULTURAL RESEARCH AND DEVELOPMENT CENTER, THE OHIO STATE UNIVERSITY, 1680 MADISON AVENUE, 44691, WOOSTER, OH

[2]DEPARTMENT OF FOOD, AGRICULTURAL AND BIOLOGICAL ENGINEERING, THE OHIO STATE UNIVERSITY, 590 WOODY HAYES DRIVE, 43210, COLUMBUS, OH

[3]HORTICULTURE AND CROP SCIENCE, OHIO AGRICULTURAL RESEARCH AND DEVELOPMENT CENTER, THE OHIO STATE UNIVERSITY, WILLIAMS HALL, 1680 MADISON AVENUE, 44691, WOOSTER, OH

RUBBER CHEMISTRY AND TECHNOLOGY, Vol. 00, No. 0, pp. 000–000 (0000)

ABSTRACT

Replacing synthetic fillers, which are commonly used to reinforce rubber, with bio-fillers has potential to improve the sustainability of rubber products. Here, eggshell (ES) (a powder with a maximum particle diameter of 9.4 μm and a median of 1.1 μm) was added to guayule natural rubber (GNR) composites to partially or fully replace bifunctionally silanized, high surface area, precipitated silica (BSS). The mixing energy consumption, mechanical properties, cross-link density, filler dispersion and final particle size, fracture surface morphology, and dyeability of GNR composites were characterized.

ES filler effectively reinforced vulcanized GNR compared with unfilled vulcanized GNR. Energy consumption, modulus at 300% strain (M300), and hardness generally decreased with increasing ES fraction (decreasing BSS), but tensile strength, gel fraction, and elongation at break increased even where cross-link density and M300 were similar. Thus, composite cross-link density was not solely influenced by silane content as the ratio and loading of ES and BSS changed. The production of the composites reduced particle size to submicron size. Even a small amount of ES improved the dispersion of BSS filler particles in the composites and hence the mechanical properties. The contributions of the two fillers to the composite properties are explained. Linear mixed models were built to predict the mechanical properties of a broader range of GNR–ES–BSS composites, and r^2 (the quality of the model predictability) was above 0.9 for all models. ES filled GNR, with or without BSS, can be dyed different colors for specific applications. The lower-cost, renewability, dyeability, and excellent performance of ES–GNR composites addresses the need for sustainable rubber products with low carbon footprint. [doi:10.5254/rct.19.81485]

INTRODUCTION

Natural rubber (NR) is one of the most important materials in the world. Although synthetic rubber is popular in numerous rubber products, NR has many advantages such as resilience, abrasion resistance, heat dispersion, and high elasticity.[1–3] The excellent mechanical properties of NR are related to strain-induced crystallization (SIC), an intrinsic characteristic of NR,[4] in which initially amorphous unstressed NR undergoes a phase transformation forming aligned polymeric crystallites under strain. The NR chains crystallize along the strain direction, which increases the strength and resistance to crack growth and deformation.[5] Owing to these distinctive characteristics, NR is irreplaceable in high performance products, such as truck and aircraft tires.[4,6,7] It is now a critical raw material, and world consumption of NR increased from 2016 to 2017.[8–12] However, the supply of NR from the Brazilian or para rubber tree (*Hevea brasiliensis*) cannot meet rising global demand.[13] Therefore, new sustainable alternative sources of NR are desired to increase NR supply. The two leading alternative rubber crops under development are guayule (*Parthenium argentatum*)[14–20] and rubber dandelion (*Taraxacum kok-saghyz*).[2,21–24]

Guayule is a perennial, drought tolerant, rubber-producing shrub native to Mexico and southwest Texas. Guayule natural rubber (GNR) and latex (GNRL) proteins do not induce latex allergies or allergic reactions related to the widespread and life-threatening Type I latex allergy caused by Hevea latex proteins.[25,26] Also, cured GNR rubber forms a larger crystallite volume,

*Corresponding author. Email: cornish.19@osu.edu

during SIC, than Hevea and rubber dandelion NR or synthetic polyisoprene rubber, which contributes to the excellent mechanical properties of GNR.[27] However, mechanical properties of unfilled and filled GNR, the effect of fillers, and polymer–filler interactions are only partially understood.[14,16–18]

Rubber fillers are commonly used to reinforce rubber composites. Carbon black (CB), the predominant and traditional rubber reinforcing nano-filler, is produced by the incomplete combustion of petroleum, an energy-intensive process that coproduces and vents large amounts of carbon dioxide.[28] An alternative to CB is bifunctionally silanized silica (BSS). When BSS is compared with CB in rubber composites like tires, it combines improved tear strength and abrasion resistance with reduced tire rolling resistance, saving energy and fuel in transportation of goods.[29] BSS can be used in combination with CB to improve crack resistance in NR composites,[30] but at high BSS concentration, the dispersion of BSS in NR is poor. When used to fully replace CB in styrene–butadiene rubber (SBR), BSS–SBR composites are more highly reinforced than with CB–SBR ones, as evinced by higher storage and loss moduli and higher complex viscosity.[31] However, like CB, BSS is neither bio-based nor renewable, and its production also indirectly causes air pollution. Although no pollution is produced during the precipitation reaction itself, the production of the sulfuric acid needed to produce silica releases SO_x, a key cause of acid rain.[32–35] In addition, silica has poor polymer–filler interaction because of its high polarity,[36] and synthetic coupling agents must be used.

Sustainable rubber reinforcing fillers, intended to fully or partially replace BSS or CB, must be available in large quantity, and composites must match or exceed current product performance. A subset of sustainable fillers also are bio-based and renewable, and their use would further improve the long-term sustainability and carbon footprint of rubber composites.[15–18,37–41] Only a few bio-based renewable fillers have the potential to generate reinforcing effects comparable to traditional fillers, such as eggshell (ES), processing tomato peel (TP), and lignin, and usually only as partial replacements of BSS or CB.[15–18,37,38]

Practically speaking, ES fillers are more accessible than TP because ES are produced year round, throughout the United States, and are simple to mechanically grind to micro-filler. The United States produced over 100 billion eggs in 2016.[39] Using an average ES weight fraction of 11% and an average egg weight of 60 g (ref. 40), about 0.7 mt/yr of ES are produced as food waste in the United States. ES waste produced by the food processing industry is mainly landfilled, which is neither economic nor eco-friendly.[41,42] ES fillers, used on a large scale, would reduce the cost and pollution of ES disposal.[43]

In this paper, ES was used to progressively replace BSS in GNR composites. The energy consumption of processing, the mechanical properties of cured composites, cross-link density, and the filler–rubber interaction of silica and ES filled GNR were investigated. Statistical models were built to predict the mechanical properties by the total filler loading and the ES fraction in the composites.

EXPERIMENTAL

MATERIALS

GNR latex was extracted from guayule shrub as described.[44] GNR was produced by drying GNR latex premixed with 1% Bostex 24 (Akron Dispersions, Akron, OH) in trays at 50°C for 120 h (HVC 70 series oven, Conceptronic Inc., Portsmouth, NH). Zinc oxide, stearic acid, sulfur, and *N*-tert-butyl-benzothiazole-sulfonamide (TBBS) were purchased from HB chemicals (Twinsburg, OH). ES were generously provided by Michael Foods (Gaylord, MN) and milled using a planetary ball mill PM 100 (Retsch, Newtown, PA) with 15 min grinding time and 500 rpm grinding speed.

TABLE I
RUBBER COMPOUND FORMULAE

Material[a]	Content, phr
GNR	100
Filler loading	50, 60, and 70
Sulfur	3.5
Zinc oxide	5
TBBS	0.75
Stearic acid	1
Antioxidant	1

[a] GNR, guayule natural rubber; TBBS, *N*-tert-butyl-benzothiazole-sulfonamide.

The milled ES were sieved to a maximum particle size of 9.4 μm (1 m^2/g surface area). The chemical composition of ES is 94% calcium carbonate, 1% calcium phosphate, 1% magnesium carbonate, and 4% organic matter (protein fibers and mucin protein).[40] Precipitated silica (PS) (Hi-Sil 190G, 195 m^2/g Brunaure–Emmett–Teller (BET) surface area, particle size was not determined) and chemically modified silica (AGILON 454GD, 140 m^2/g BET surface area) were the generous gift of PPG Industries, Inc. (Monroeville, PA). Silane coupling agent (Bis[3-(triethoxysilyl)propyl] tetrasulfide, SCA98) was generously provided by Struktol Company of America (Stow, OH). Antioxidant (Bostex 24) was generously provided by Akron Dispersions (Copley, OH). Green rubber composites were made by adding 0.5 phr of green pigment (GM Foam, Inc., Van Nuys, CA) during compounding. Orange rubber composites were made by adding 1 phr orange pigment (E-6580, Akrochem Corp., Akron, OH) and 2 phr rutile TiO_2 (Rutile Titanum Dioxide, Akrochem Corp.) during compounding.

SAMPLE PREPARATION

In a preliminary experiment, GNR was compounded with 50 phr chemically modified silica or with 50 phr PS + 4.5 phr silane, according to the protocols detailed below. The 50 phr PS + 4.5 phr silane filled GNR had higher tensile strength, modulus at 300%, but lower elongation at break than 50 phr chemically modified silica. These properties indicate that the silanization reaction was complete, and because the reinforcement was better than chemically modified silic, we chose the combination of PS and silane as the BSS filler in this research.

GNR was compounded with fillers, pigments, and curing agents (zinc oxide, stearic acid, sulfur, and TBBS) in a Banbury mixer (100°C, 6.3 rad/s, Farrel-Birmingham Co., Buffalo, NY), with a fill factor of 0.45–0.51. The composition details are shown in Tables I and II. Three different filler loadings of 50, 60, and 70 phr were used. In each filler loading, ES replaced PS from 0 to 25%, 50%, 75%, and 100% (Table II). In order to improve silica–GNR interaction, BSS was produced by silane coupling agent (9% of PS by weight) and PS. The filler loading and ES fraction were measured by weight instead of volume, since both BSS and ES are essentially mineral fillers. Green and orange pigments were added to compounds during mixing to assess the dyeability of the GNR composites. During compounding, energy consumption was recorded by a Pro-server Ex software v 1.3 (Pro-face Digital Electronics CO, Osaka, Japan). For each compound, GNR and fillers (ES, BSS, and silane coupling agent) were compounded in the Banbury mixer with 60 rpm rotor speed and starting temperature of 80°C for 12 min. Then sulfur, zinc oxide, TBBS, stearic acid, antioxidant, and pigment were added to each compound and mixed at 60 rpm for 3 min. The

TABLE II
RUBBER FILLER COMPOSITION

	ES fraction, %				
Filler loading[a]	0	25	50	75	100
50 filler loading					
ES content, phr	0	12.5	25	37.5	50
PS fraction, %	100	75	50	25	0
PS content, phr	50	37.5	25	12.5	0
Silane content, phr	4.5	3.4	2.3	1.1	0
60 filler loading					
ES content, phr	0	15	30	45	60
PS fraction, %	100	75	50	25	0
PS content, phr	60	45	30	15	0
Silane content, phr	5.4	4.1	2.7	1.4	0
70 filler loading					
ES fraction, %	0	25	50	75	100
ES content, phr	0	17.5	35	52.5	70
PS fraction, %	100	75	50	25	0
PS content, phr	70	52.5	35	17.5	0
Silane content, phr	6.3	4.7	3.2	1.6	0

[a] ES, eggshell; PS, precipitated silica.

compounding temperature increased from 80°C at the beginning of the mixing to temperatures of 102°C–123°C when the compound was dumped from the mixer. After compounding, the samples were milled using a two-roll mill (roll diameter 15.24 cm and roll width 33.02 cm) (Rubber City Machinery Corp., Akron, OH), and each compound passed through the mill nine times. The composites were cured as sheets with a thickness of 2 mm according to ASTM D3182, for 12 min under 160°C and 16 tons of force[45] then stored at ambient temperature for at least 24 h before testing.

SWELLING TESTS

Swelling measurements were performed on samples of 10 mm × 10 mm × 2 mm. The initial weight of the dry samples was recorded to an accuracy of 0.1 mg. Samples were immersed in toluene at 25°C for 96 h, with the solvent being replaced by fresh solvent every 24 h during the swelling period, according to ASTM D6814.[46] Excess solvent was decanted, and the samples were blotted and weighed. The swollen sample was fully dried at 100°C for 24 h and reweighed.

The cross-link density was calculated by the Flory–Rehner equation:[47]

$$-\ln(1 - V_r) - V_r - \chi V_r^2 = V_s \eta_{\text{swell}} \left(V_r^{\frac{1}{3}} - \frac{V_r}{2} \right)$$

χ is the polymer–solvent interaction parameter and V_r is the volume fraction of the rubber in swollen gel. For GNR–toluene, χ is 0.391 (ref. 46). η_{swell} is the cross-link density of rubber (kmol/m^3). V_s is the molar volume of toluene (106.27 cm^3/mol) (ref. 48).

The cross-link density, V_r was calculated using the equation

$$V_r = \frac{V_{\text{rubber}}}{V_{\text{solvent}} + V_{\text{rubber}}} = \left(\frac{m_d - m_b \times f}{\rho_{\text{rubber}}}\right) \div \left[\frac{m_s - m_d}{\rho_{\text{solvent}}} + \left(\frac{m_d - m_b \times f}{\rho_{\text{rubber}}}\right)\right]$$

In Eq. 2, m_b, m_s, m_d are the weights of the sample: m_b is before swelling, m_s is swollen weight, and m_d is dry weight measured after drying the swollen samples. The parameters ρ_{rubber} and ρ_{solvent} are the density of GNR and toluene. The parameter ρ_{rubber} was 0.92 g/cm^3, which was measured using an analytical balance (Model ME54E, Mettler Toledo, Columbus, OH); ρ_{solvent} was 0.867 g/cm^3; and f is the weight fraction of non-rubber components. Gel fraction was calculated by the weight of the dried sample (m_d) divided by the initial weight (m_b).

MECHANICAL PROPERTY TESTS

Evaluation of the tensile mechanical properties of the cured composites was performed using a tensiometer (Model 3366, Instron, Norwood, MA) following ASTM D 412 (ref. 49) at room temperature (~21°C). Before tensile tests, each dumbbell shaped specimen was cut using an ASTM D412 Die C.[49] The modulus at 300% strain (M300) was represented by the tensile stress at 300% strain. The tensile strength was calculated by the tensile force divided by the cross-sectional area of the middle part of the dumbbell samples. A high elongation axial extensometer (Model 3800, Epsilon Technology Corp., Jackson, WY) was used to calibrate the strain value determined by the tensiometer. Hardness was determined according to ASTM D 2240 (ref. 50) using a Shore A durometer (Model 408, PTC Instruments, Los Angeles, CA) with an operating stand type 2 (Model 472, PTC Instruments, Los Angeles, CA). At least three samples of composites made from each formulation were tested.

SCANNING ELECTRON MICROSCOPY

The morphology of ES (without milling) and micro-sized ES were observed and imaged using a scanning electron microscope (SEM; Hitachi S-3500N, Tarrytown, NY) with an accelerating voltage of 15 kV. Samples were coated with platinum before SEM measurements at ambient temperature (21°C). The size distribution of 300 representative ES particles in the ES powder were analyzed with JMP Pro 12 software (SAS Institute Inc., Cary, NC).

The tensile ambient fracture and cryogenic fracture surfaces were observed by SEM. The GNR composites exhibited a "plastic" state in liquid nitrogen, which maintained the filler dispersion within the rubber matrix at the fracture surface. Cryogenic fracture surfaces were prepared by immersing untested dumbbell samples in liquid nitrogen for 4 min. Then samples were broken in liquid nitrogen (–196°C). The ambient tensile fracture surfaces were prepared from the broken samples of tensile tests. The broken regions with 5 mm height were cut, and fracture surfaces were on top. Fracture surfaces were washed with 70% ethanol and coated with platinum before SEM measurements at ambient temperature. Surfaces were observed and imaged using a SEM (Hitachi S-3500N) with an accelerating voltage of 15 kV. The size of filler particles and agglomerates on cryogenic fracture surfaces were analyzed with JMP Pro 12 software (SAS Institute Inc.).

DYEABILITY

Colored composites made with 12.5 phr ES and 37.5 phr BSS were compared with 50 phr CB-filled GNR by placing sample dumbbells onto a white paper background. Lab color space parameters were used to compare differences between samples. Adobe Photoshop CS5 (Adobe Systems Inc., San Jose, CA) was used to analyze the different colors.

TABLE III
PARAMETER NOTATIONS OF THE LINEAR MIXED STOCHASTIC MODEL

Independent variables/response variables	Physical meaning (units)
x_1	Eggshell fraction (%)
x_2	Filler loading (phr)
Y_1	Tensile strength (MPa)
Y_2	Elongation at break (%)
Y_3	Modulus at 300% strain (MPa)
Y_4	Hardness number
a, b, and c	Constants

STATISTICAL ANALYSES

The power consumption required to mix the different composite compounds was statistically analyzed and compared using Tukey tests by JMP Pro 12 software (SAS Institute Inc.). Two different statistical models (linear and linear mixed) were used to predict the mechanical properties (tensile strength, elongation at break, M300, and hardness) of ES and BSS filled GNR composites and the model with highest r^2 (the quality of the model predictability)[51,52] and significance was identified for further use (see Table III for parameter notations). Analyses of variance (ANOVA) were used to determine the importance and significance of each parameter to the model. Significance levels were 0.05 for all analyses. Minitab v.17 (Minitab Inc., State College, PA) was used for the regression analyses.

$$\frac{x_2}{Y_i} = a + bx_1 + cx_2 i = 1, 2, 3, 4$$

RESULTS

POWER CONSUMPTION

As would be expected, increasing filler loading, especially at the higher BSS proportions, required greater amounts of power to complete the compound mixing (Table IV). However, at all loadings, the replacement of BSS by ES significantly reduced the power consumed during mixing of the GNR compounds (Figure 1; Tables IV and V),[21] and in general, as the ES fraction increased, the relative energy savings also increased. The power savings achieved, when entirely replacing BSS with ES, increased with loading level, saving 31, 34, and 39% at 50, 60, and 70 phr ES filler, respectively (Table V). When the amount of ES filler matched or exceeded the BSS loading, the power consumption differences with loading decreased, and very little difference was apparent between 60 and 70 phr (Figure 1 and Table IV). All loadings of 100% ES had similarly low power requirements to effectively mix these compounds.

SWELLING TESTS

The cross-link densities of GNR composites with 50 and 60 phr filler loading changed little as ES fraction increased from 0 to 25% (Figure 2). However, cross-link densities decreased with increasing ES fraction from 25 to 100%. At 70 phr, the cross-link density monotonically decreased

TABLE IV
POWER REQUIRED TO ACHIEVE COMPLETE COMPOSITE MIXING, ORDERED BY POWER CONSUMPTION

Filler composition (phr + filler type)[a]	Significance differences	Mean power consumption, kw
70 PS	A	19.33
60 PS	B	18.20
52.5PS 17.5ES	C	16.97
50 PS	D	16.45
45PS 15ES	E	15.65
37.5PS 12.5ES	F	14.75
35PS 35ES	F	14.66
30PS 30ES	F	14.36
25PS 25ES	G	13.32
17.5PS 52.5ES	G H	12.90
15PS 45ES	H	12.64
60ES	I	11.98
70ES	I J	11.88
12.5PS 37.5ES	I J	11.66
50ES	J	11.43

[a] ES, eggshell; PS, precipitated silica. (Different letters represent significantly different power consumption levels determined by Tukey tests. Each power consumption value is the mean of real-time power consumption.)

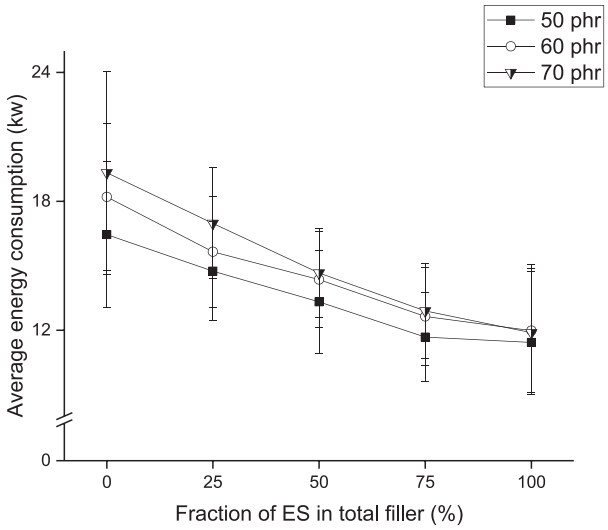

FIG. 1. — The average power consumed to complete mixing of GNR compounds with different loadings and ratios of eggshell (ES) and precipitated silica fillers. Each value is the mean of 3 ± standard deviation.

TABLE V
THE PROPORTION OF SAVED ENERGY TO ENERGY CONSUMPTION DURING COMPOUNDING OF GUAYULE RUBBER COMPOSITES MADE WITH EGGSHELLS AND SILICA

		ES weight fraction in filler, %				
Energy saving ratio, %[a]		0	25	50	75	100
Filler loading ES + BSS (phr)	50	0	10	19	29	31
	60	0	14	21	31	34
	70	0	12	24	33	39

[a] Saved energy was calculated as the percentage of energy consumed during mixing compared with precipitated silica–eggshell filled guayule natural rubber.

at all levels of BSS replacement by ES. The greatest cross-link densities in mixed filler composites were obtained at 60 phr loading, but at 70 phr when BSS was the only filler used. Filler loading had little effect on cross-link density at 100% ES fraction. Gel fraction slightly increased with increasing ES and decreasing BSS and slightly increased with filler loading (Figure 3).

MECHANICAL PROPERTIES

The tensile strength of GNR composites reinforced by ES and BSS generally increased with increasing fraction of ES (Figure 4) with maximum strength achieved in 60 phr of ES alone. At the lower ES fractions, tensile strength was inversely related to loading level, and only at 50 phr loading did tensile strength plateau at 50% ES. Elongation at break increased with increasing ES fraction and was inversely related to loading (Figure 5). The elongation at break of 60 phr ES and BSS filled GNR was little affected at high ES fraction. The maximum value of elongation at break was at 50 phr ES filled GNR. In contrast to tensile strength and elongation at break, M300 decreased with increasing ES fraction (Figure 6). M300 increased with increasing filler loading, which is more significant at lower ES fractions. Similar to M300, hardness increased with filler loading and

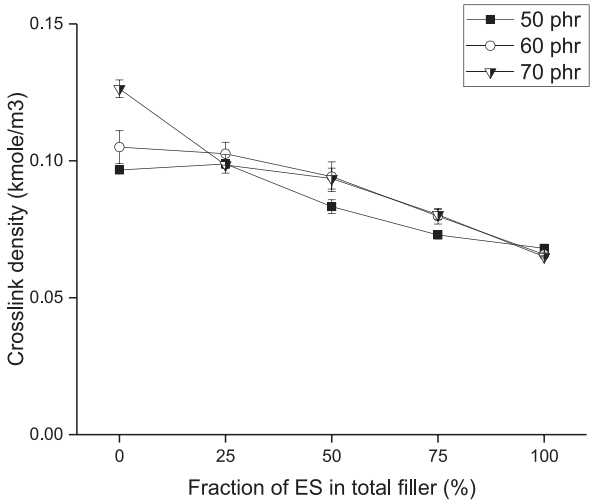

FIG. 2. — The cross-link density of GNR composites with different loadings and ratios of eggshell (ES) and precipitated silica fillers. Each value is the mean of 3 ± standard deviation.

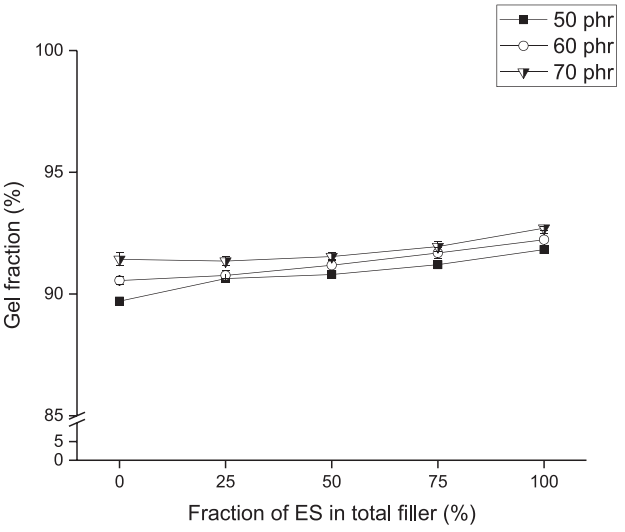

FIG. 3. — The gel fraction of GNR composites with different loadings and ratios of eggshell (ES) and precipitated silica fillers. Each value is the mean of 3 ± standard deviation.

decreased with increasing fraction of ES (Figure 7). Hardness did, however, reach a minimum hardness while BSS was still present at all total loading levels. All filled samples had higher strength, modulus, and hardness than unfilled GNR.[18]

SCANNING ELECTRON MICROSCOPY

ESs have high porosity, developed to support the high gas exchange needed for developing chicks to respire efficiently,[16,53] and this structure caused high irregularity of micro-ES after ball

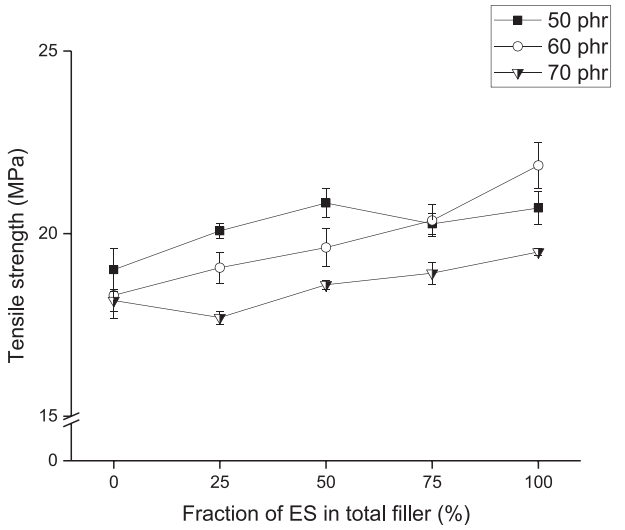

FIG. 4. — The tensile strength of GNR composites with different loadings and ratios of eggshell (ES) and precipitated silica fillers. Each value is the mean of 3 ± standard deviation.

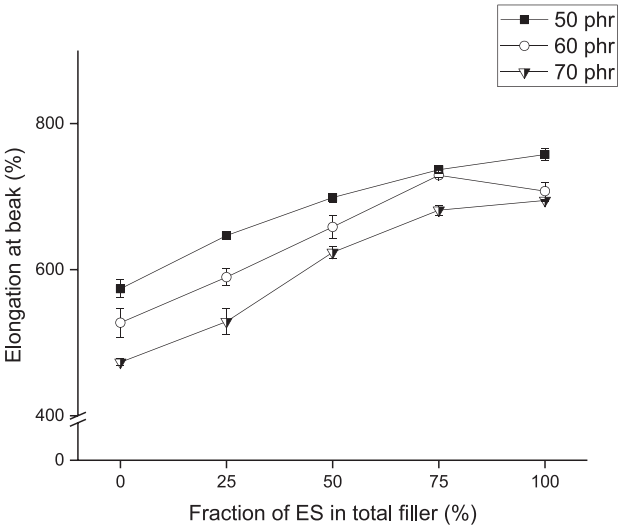

FIG. 5. — The elongation at break of GNR composites with different loadings and ratios of eggshell (ES) and precipitated silica fillers. Each value is the mean of 3 ± standard deviation.

milling (Figure 8). The ES powder had a maximum particle size of 9.4 μm, and a mean diameter of 1.3 μm (Figure 9), but most particles were smaller than 2 μm, with a considerable subfraction in the nano range.

Composites with a total filler loading of 50 phr were selected to visualize the filler–rubber interactions of GNR composites reinforced by ES and BSS fillers at the fracture surfaces of composites caused by tension breakage. The more highly loaded composites were not evaluated by SEM because they all showed similar trends in their mechanical properties to the 50 phr versions (Figures 4–7). Composites solely filled with BSS had agglomerated filler particles and cavities in

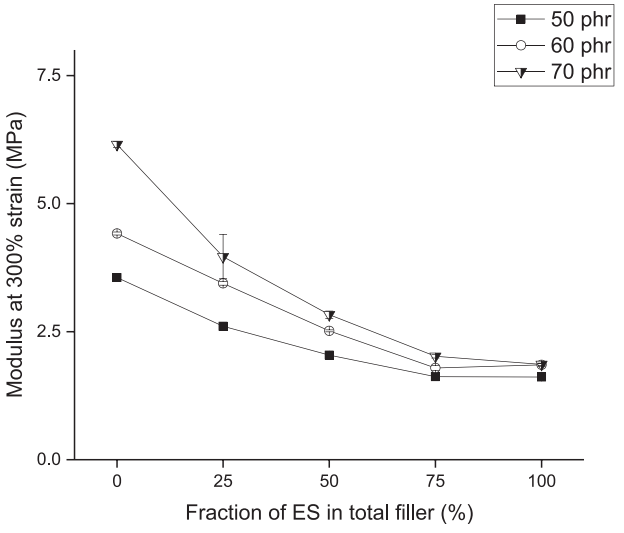

FIG. 6. — The M300 of GNR composites with different loadings and ratios of eggshell (ES) and precipitated silica fillers. Each value is the mean of 3 ± standard deviation.

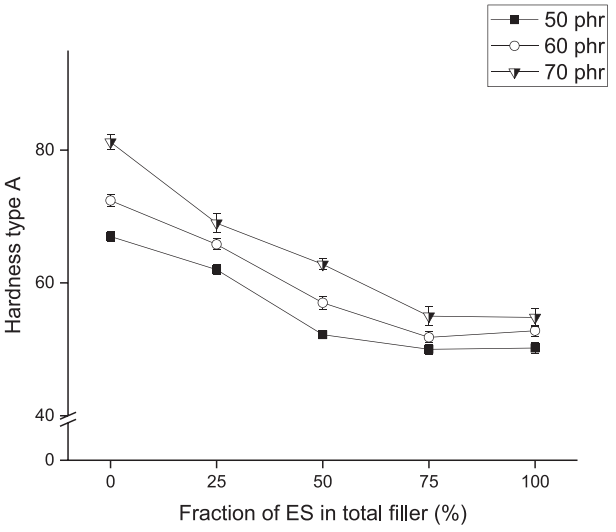

FIG. 7. — Hardness (Shore A) of ES and BSS filled GNR with different loadings and ratios of eggshell (ES) and precipitated silica fillers. Each value is the mean of 3 ± standard deviation.

the polymer matrix (Figure 10a) at the fracture surfaces. These cavities indicated that the filler particles were poorly bound to the polymer matrix (a poor rubber–filler interaction) even though a coupling agent was used to improve the interaction. In contrast, "bridge" structures were observed in GNR composites containing ES filler (Figure 10b,c), indicating an intimate polymer–filler interaction.

Although all loadings showed similar trends, the cryogenically fractured surfaces of 60 phr filler loaded GNR composites were visualized because these included the highest performing samples (Figure 11). The ES particles were smaller and more uniformly dispersed (Figure 11c) than the BSS particles (Figure 11a). In addition, the ES filler appeared to reduce the BSS agglomerate particle size, improving the BSS dispersion in the mixed filler composite (Figure 11b). Filler agglomerates were smaller in the ES–GNR composite (mean particle size = 0.295 μm) than the BSS filled one (mean particle size = 0.474 μm) (Figure 12). The mean particle size was smallest (0.154 μm) in the composites with equal parts of both fillers (Figure 12), suggesting that not only does the ES filler significantly improve the dispersion of the BSS filler but that the BSS filler may also improve the dispersion of ES. It also is clear that the mixing and milling operations reduced the ES

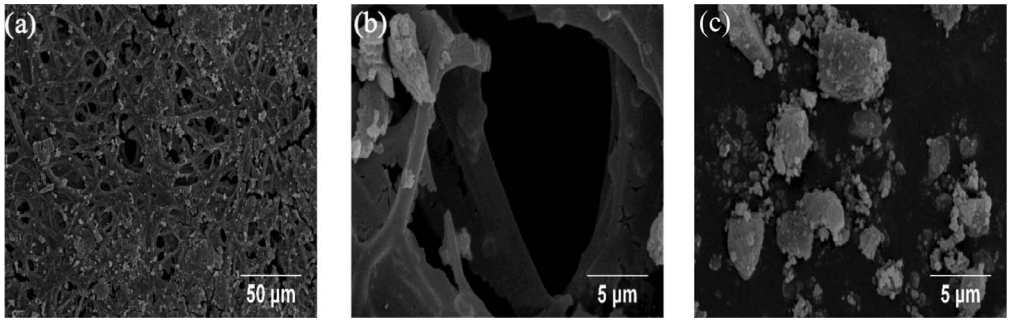

FIG. 8. — SEM pictures of ES. (a) Eggshells at low magnification (500×); (b) Eggshells at high magnification (5000×); (c) Micro-sized ES at high magnification (5000×).

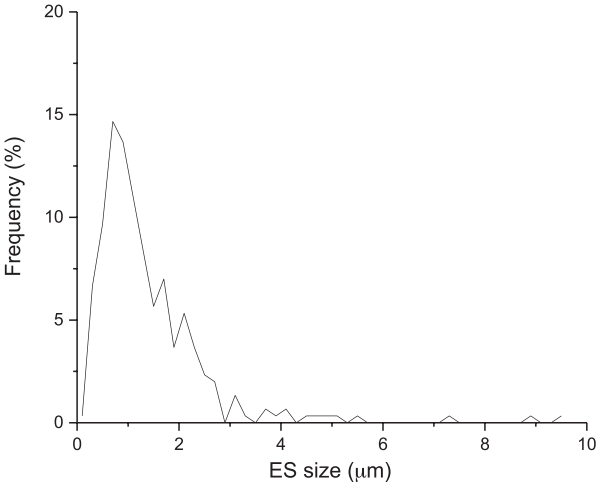

FIG. 9. — Size distribution of ES before compounding (median, 1.084 μm; mean, 1.391 μm).

particle size considerably below what was measured in the powder itself (mean particle diameter of 1.3 μm).

DYEABILITY

The ES and BSS filled GNR composites made with orange and green pigments were distinctly colored compared with a CB-filled GNR composite (examples in Figure 13). The LAB values define the different colors made by adding the different pigments into GNR compounds (Figure 13).

STATISTICAL ANALYSIS

The ANOVA showed that the coefficients in each model were significant ($p < 005$) (data not shown) and that the R^2 in all models were above 0.9 (Table VI). The linear mixed stochastic model (Eq. 3, Tables III and VI, and Figure 14), best predicted the mechanical properties (tensile strength,

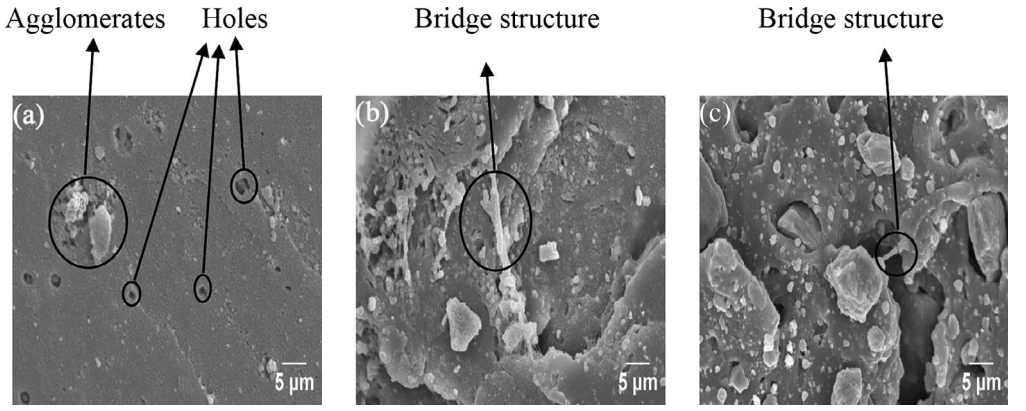

FIG. 10. — Scanning electron microscopy photographs of tensile fractured surface of guayule natural rubber composites with 50 phr filler loading. (a) 50 phr precipitated silica–filled guayule natural rubber; (b) 25 phr precipitated silica and 25 eggshell filled guayule natural rubber; (c) 50 phr eggshell filled guayule natural rubber.

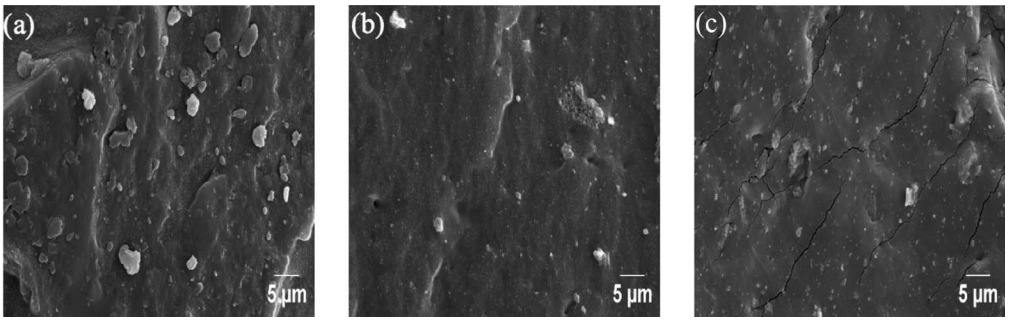

FIG. 11. — SEM pictures of cryogenically fractured surfaces of guayule natural rubber composites with 60 phr filler loading. (a) 60 phr precipitated silica–filled guayule natural rubber; (b) 30 phr precipitated silica and 30 phr eggshell filled guayule natural rubber; (c) 60 phr eggshell filled guayule natural rubber. The filler particles appear as lighter dots in the darker gray rubber matrix because of the different conductivity of the fillers and the rubber matrix.

elongation at break, M300, and hardness) of the GNR composites. All parameters significantly contributed to the mechanical properties predictive model. The observed data points were distributed close to the predicted value (Figure 14).

$$\frac{x_2}{Y_i} = a + bx_1 + cx_2 i = 1, 2, 3, 4$$

DISCUSSION

Reinforcing effects of fillers are generally evaluated by the increment of increased stiffness and strength of the rubber matrix compared with unfilled rubber, until too much filler is loaded and the material fails.[54] Filler-induced reinforcement commonly would lead to higher gel fraction, cross-link density, modulus, hardness, and tensile strength with a lower elongation at break compared

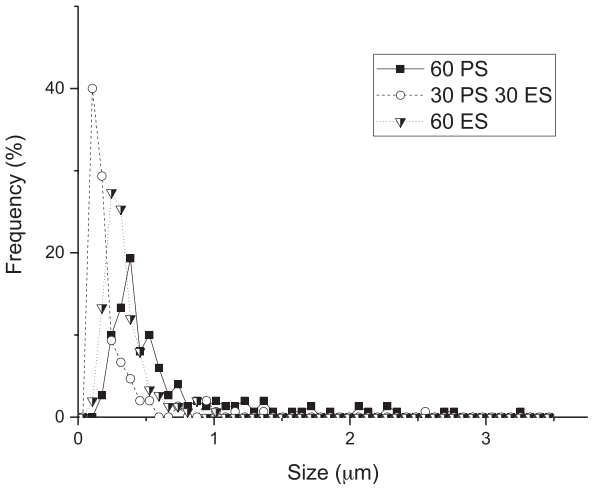

FIG. 12. — Size distribution of filler in GNR composites with different ES fraction. 60 phr BSS filled GNR composites (median, 0.474 μm; mean, 0.681 μm), 30 phr BSS and 30 phr ES filled GNR composites (median, 0.154 μm; mean, 0.244 μm), 60 phr ES filled GNR composites (median, 0.295 μm; mean, 0.335 μm,).

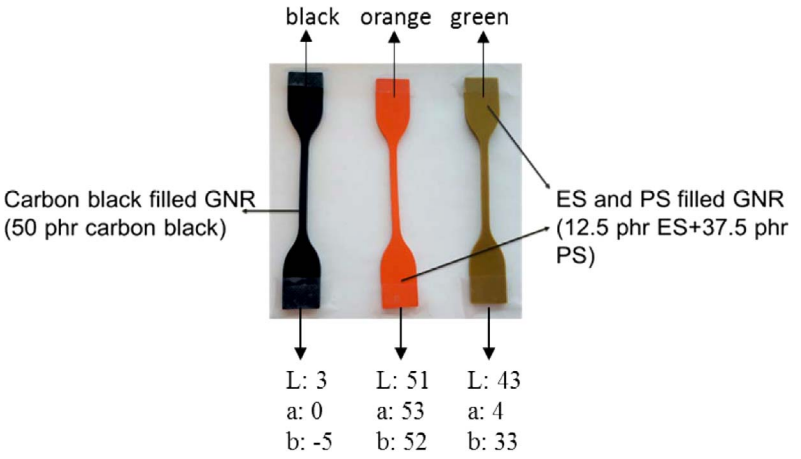

FIG. 13. — Dyed eggshell and precipitated silica–filled guayule natural rubber composites with a carbon black–filled comparison.

with unfilled rubber. In contrast, diluent fillers used as polymer extenders would be expected to decrease gel fraction, cross-link density, tensile strength, and elongation at break, but increase modulus and hardness. Increasing loading generally increases these effects until material failure is approached as the loading becomes too high to sustain material integrity.

It has been argued that the primary indicator of composite reinforcement is modulus, which is determined by cross-link density and, in turn, that silane concentration is the sole modulator of cross-link density. In this study, several composites were identified with very similar cross-link densities, namely, 25% and 50% ES fraction with 70 phr filler loading, 50% ES fraction with 50 phr filler loading, and 75% ES fraction with 60 phr loading. Clearly, the wide range of silane concentration in these composites did not cause different cross-link densities in the GNR composites.

The reinforcing effect of ES was demonstrated by dramatic increases in tensile strength, M300, and hardness number, with reduced elongation at break, compared with unfilled GNR. Composites made with PS, a known reinforcing filler, behaved similarly to ES–GNR composites with filler loading from 0 to 70 phr (Figures 4–7 and Table VII). Apart from tensile strength (Figure 4), which was higher in 100% ES than in 100% BSS GNR composites, GNR was reinforced more by BSS than ES (Figures 2, 6, and 7).

The interaction of the two fillers and the GNR in composites made with different ratios and loadings of the two fillers directly affected final properties. In general, the increasing gel fraction, tensile strength, and elongation at break (Figures 3–5) coupled with decreasing cross-link density,

TABLE VI
PREDICTIVE MODELS FOR INDIVIDUAL MECHANICAL PROPERTIES

Response variable	Predicted model[a]	R^2
Tensile strength, MPa	$Y_1 = x_2/(-0.567 - 0.00311x_1 + 0.06368x_2)$	0.9677
Elongation at break, %	$Y_2 = x_2/(-0.023 - 0.00033x_1 + 0.00234x_2)$	0.9342
M300, MPa	$Y_3 = x_2/(13.479 + 0.21682x_1)$	0.9164
Hardness number, Shore A	$Y_4 = x_2/(0.211 + 0.00353x_1 + 0.01036x_2)$	0.9107

[a] x_1, eggshell fraction (%); x_2, filler loading (phr).

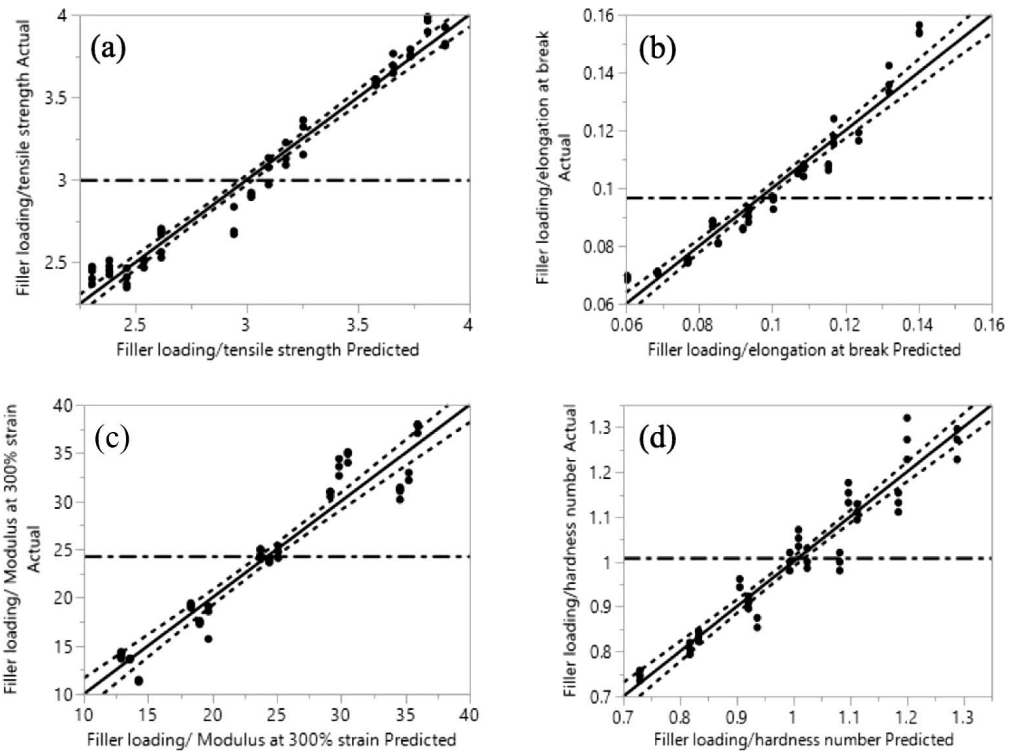

FIG. 14. — Experimental vs values predicted by the mixed linear models. (a) Filler loading/tensile strength; (b) filler loading/elongation at break; (c) filler loading/modulus at 300% strain; (d) filler loading/hardness number. The solid line is the regression line; dashed lines are the 95% confidence intervals; the dash-point line is the average of observed values; the solid circles are observed values.

modulus, and hardness (Figures 2, 6, and 7) caused by increasing ES fraction was similar to that reported previously when CB, not PS, was partially replaced by ES in GNR composites.[17,18]

The gel fraction represents the weight percentage of insoluble parts after toluene extraction. Higher gel fraction resulted from higher filler loading, since fillers (ES and BSS) are insoluble in toluene (Figure 3). The chemical cross-linking of the rubber molecules by sulfur should be essentially the same in all composites because the concentrations of cross-linking agent and sulfur were identical. Therefore, the higher gel fraction in composites made with ES (Figure 3) must result from a stronger ES and GNR non-covalent interaction than that between BSS and GNR. ES filler

TABLE VII
THE MECHANICAL PROPERTIES OF GUAYULE NATURAL RUBBER

Filler type[a]	Tensile strength, MPa	Elongation at break, %	M300, MPa	Hardness number, shore A
Unfilled[18]	7	1581	0.98	37
50 phr ES	21	758	1.61	50
60 phr ES	22	707	1.85	53
70 phr ES	20	695	1.86	55

[a] ES, micro-sized eggshell filler.

particles may act as physical cross-linking points (Figure 10b,c) impeding the mobility of GNR molecules during the swelling tests and their solubility during immersion in toluene. This is independent of the much larger increase in cross-link density caused by the PS–silane–GNR covalent bonds, which are directly proportional to the BSS. The cross-link density increased as filler loading increased from 50 to 60 phr, which is due to more PS–silane–GNR covalent bonds being formed. The additional cross-linking structures formed by PS–silane–GNR covalent bonds may also explain that the cross-link density of GNR composites with 100% BSS increased as filler loading increased from 60 to 70 phr. However, the cross-link density of GNR composites with mixed fillers changed little as filler loading increased from 60 to 70 phr, which is due to the balance between PS–silane–GNR covalent bonds and BSS agglomeration. Silica silanization may be hindered by BSS agglomeration at high loadings because only the surface of the agglomerates can interact with the silane, and this would reduce cross-link density.

High cross-link density (Figure 2) is directly tied to the increased M300 and hardness observed (Figures 6 and 7). In addition, strong silica networks may explain the higher M300 and hardness of BSS–GNR than ES–GNR, as rubber molecules are trapped and immobilized within the expanding BSS filler networks in the composites, as the effective filler volume fraction, hardness, and modulus increase. Such effects can be modified by filler loading, for example, 15 phr ES and 45 phr BSS reinforced GNR composites had a similar M300 to GNR with 50 phr BSS (Figure 6).

PS inherently has a poor rubber–filler interaction, due to its higher polarity than ES. Previous studies reported that carbon black is more polar than ES[15] and that PS is more polar than CB.[55,56] This incompatibility has been addressed in silica-filled synthetic rubber composites[57] by use of silane coupling agents, such as Bis[3-(triethoxysilyl)propyl] tetrasulfide. This agent has tetrasulfane groups that react with the double bonds in the rubber molecules, and ethoxy groups that react with PS (Figure 15a,b). Several reports demonstrate that silanization reactions occur between 60°C and 120°C, which includes the compounding temperature range we used in our research.[58–60] It was also reported that the silica modification is complete in 8 min compounding time at 110°C chamber temperature.[61] Our mixing time was set at a constant 13 min, which was a minimum of 9 min after the power consumptions stabilized for all compounds, so silanization would be complete. However, silane coupling agents work less well in Hevea NR than in synthetic rubber,[34,36] probably because some silane coupling agents react with the nonrubber components (proteins, fatty acids, and resins) instead of the NR.[34,62] The relatively poor reinforcing effect of BSS on Hevea NR was also matched here in the BSS–GNR composites where BSS particles debonded from the rubber matrix leaving cavities (Figure 10a).[37,63] Also, some of the higher polarity nonrubber components in GNR may absorb onto the silica particle surface during mixing, which would inhibit reactions between silica and the coupling agent, reducing the efficiency of the coupling agent.

The increased elongation at break and tensile strength with increasing ES fraction may be due to the differences in SIC in ES–GNR and BSS–GNR. Much stronger SIC was demonstrated in ES–GNR stress–strain curves than BSS–GNR (Figure 16a) and by the higher derivative of stress with respect to strain (Figure 16b) at all loadings. The inhibition of SIC development in the BSS–GNR composite is due to the PS–silane–NR covalent bonds, which restrict the movement of rubber polymers impeding their alignment into crystallites. The more pronounced SIC observed in the ES–GNR composites occurs because the rubber molecules are more mobile,[64] allowing considerably more elongation of the composites, alignment into crystallites and higher strength immediately before the break point. Thus, as ES fraction increases in the composites, greater SIC development occurs, leading to the higher tensile strength (Figure 4) and elongation at break (Figure 5) observed.

In addition, the bridge structures, which occur in ES–GNR but not BSS–GNR (Figure 10b,c), indicate a better interaction of GNR with ES than BSS, which would also contribute to the observed higher strength (Figure 4). Similar bridge structures were reported when ES was mixed with CB

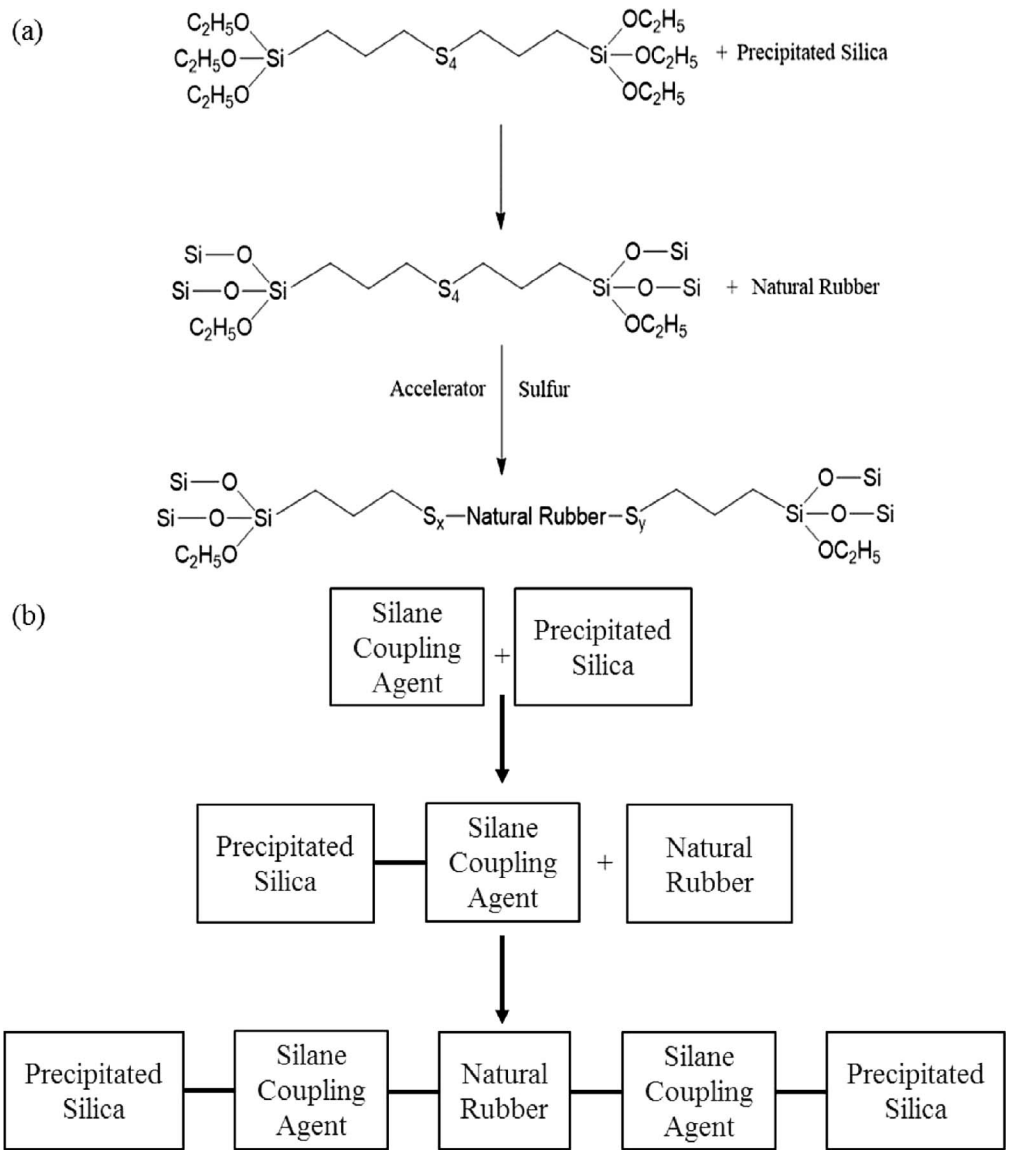

FIG. 15. — Reactions between silane coupling agent, natural rubber molecules, and precipitated silica. (a) Chemical reaction; (b) schematic diagram of additional cross-linking structure.

filler in GNR composites, and they were interpreted to mean that the better adherence of ES particles to rubber molecules absorbed stress transferred from the rubber molecules to the ES–GNR bridges under strain.[18] The tensile strength of the 50 phr composites plateaus at 50% ES, and additional replacement did not affect tensile strength, indicating that the physical interaction of ES with GNR is very similar to the combined physical and chemical interaction of BSS with GNR.

In addition to the stronger rubber–filler physical interaction of GNR with ES than PS, filler dispersion is essential to mechanical properties. Filler agglomerates formed at 70 phr filler loading negatively impact the tensile strength (Figure 4) through the formation of failure points and crack propagations sites, as was also seen at lower total filler loading with high BSS (Figure 10). More

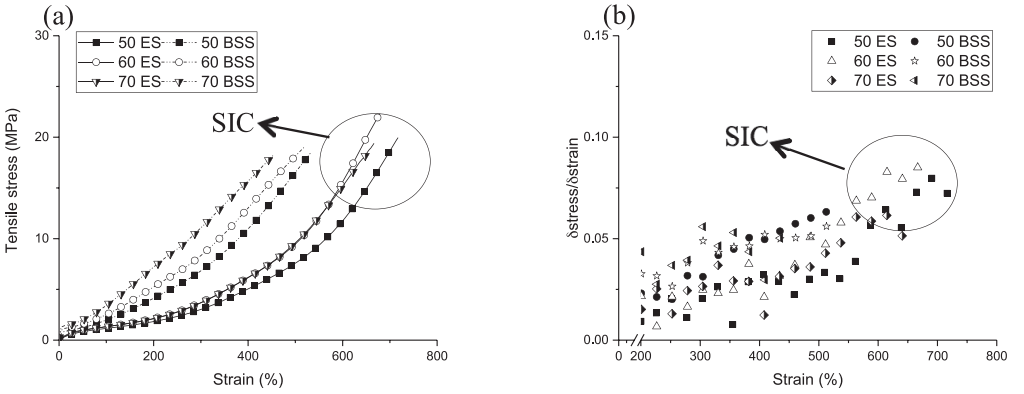

FIG. 16. — Stress–strain cures for 0 and 100% eggshell filled guayule natural rubber composites. (a) Stress–strain curves; (b) derivative of stress with respect to strain–strain cures.

uniform dispersion and smaller size also contributed to the greater strength of GNR composites containing ES. Interestingly, ES particles appeared to help de-agglomerate and disperse the BSS particles when both fillers were present, with a smaller reciprocal effect of BSS reducing ES particle size (Figures 10–12). As ES is added, the ES reduces the amount of BSS agglomeration, with concomitant increases in tensile strength and elongation at break. However, at even high total filler loadings, even more ES is needed to disperse the BSS filler, and this explains the increased tensile strength achieved in 60 and 70 phr composites with more than 50% ES. Filler agglomerates for failure points and crack propagations sites formed at high filler loading may also negatively impact the elongation at break (Figure 5). Although the PS used in this research has a larger apparent surface area (195 m^2/g, BET surface area[65]) than ES (1 m^2/g BET surface area[15]), the agglomerates observed by SEM reduce the actual BSS surface area substantially, and the actual interfacial area between BSS and GNR molecules was smaller than between ES and GNR.[15,65] This is because the actual interfacial area between BSS or ES and the rubber matrix was not the same as the surface area determined by nitrogen absorption (BET) due to the high irregularity ES particles (Figure 8).

The 100% BSS filled GNR compound required over 30% more mixing energy than 100% ES–GNR at all three loadings (Figure 1 and Table V). BSS fillers with high specific surface area are known to form strong agglomerates, mediated by hydrogen bonds between the surface silanol groups,[55] and it is likely that these are only disrupted by extensive mixing. ES filler reduced the power consumption required to compound GNR when partially or completely replacing BSS because the BSS was de-agglomerated by ES, which interfered with the formation of BSS filler networks. When more than 50% BSS (or 57% CB[17]) was replaced by ES, 19% less power was used. This has a concomitant carbon benefit because 65% of U.S. electricity is generated from fossil fuels (34% natural gas, 30% coal, and 1% petroleum).[66]

The linear mixed stochastic models predicted most of the variation in four different response variables (Table VI; Figure 14). Thus, these models can be used to easily determine the specific filler composition needed to achieve desired mechanical properties, which may help rubber manufacturers with product design.

The dyeability of rubber products is constrained by the type of rubber filler. Most rubber products are black, because CB is used as filler, and black is difficult to change to other colors. Although PS-filled rubber composites can be dyed different colors, nonrenewability limits the sustainable development of BSS as rubber filler. GNR–ES composites were dyed orange and green

(Figure 13) and seem to have comparable dyeability to GNR BSS composites, which is an advantage over CB in some markets.

In addition to the excellent reinforcement provided by hybrid ES–PS filler, the use of ES to replace synthetic fillers can also reduce the cost of rubber products. As a food industry waste, an ES-filler producer may obtain ES at zero cost or even be paid to take them. Nearly 90% of U.S. ES waste is produced at food industry and retail businesses (grocery stores and restaurants).[67] Egg processing facilities are widely distributed and are many more than PS or BSS suppliers, indicating that ES could become a very accessible material.

In the laboratory (with no economies of scale), the power consumption of milling ES into microscopic size was 1.25 kWh per 600 g ES, and electricity was about \$0.12 per kWh, leading to an ES cost of approximately \$250/ton. Thus, on a producer scale, it is likely that ES ($<$9.4 μm) could be produced much more cheaply than PS (\$500–800/ton) or CB (\$720–730/ton).[68–70] The inclusion of ES fillers in rubber composites would reduce landfill loading, further supporting their environmentally friendly footprint compared with synthetic fillers.

GNR composites with BSS and ES satisfy the physical requirements for automotive applications, rubber sheet gaskets, and rubber tapes according to ASTM D2000, D1330, and D4388.[71–73] Guayule natural rubber does not induce latex allergy.[26,74] Egg allergies are primarily to the egg proteins, and the proteinaceous membrane was completely removed before compounding, so the GNR–ES composites should have low risk for people allergic to eggs.

CONCLUSION

Partial or complete replacement of BSS with ES can improve mechanical properties of GNR composites suitable for commercial applications. In addition, sustainability, energy consumption, and cost of rubber production can be improved by producing GNR rubber products containing renewable and easily made ES, and filler applications create value for ES wastes generated by the food industry. The replacement of BSS with ES may also be applied to other natural and synthetic rubbers. Additional improvements may be achieved by ES surface modifications and create new elastomeric materials.

ACKNOWLEDGEMENT

Funding: This work was supported by the Ford Motor Company, Dearborn, MI (OSU-Ford Alliance grant number 60059609), and the U.S. Department of Agriculture, National Institute of Food and Agriculture (Hatch project 230837). Also, we thank PPG Industries, Struktol Company of America, Akron Dispersions, and Akrochem for donating research materials.

REFERENCES

[1]S. Prasertsri and N. Rattanasom, *Polym. Test*. **30**, 515 (2011).

[2]Y. Nie, Z. Gu, Y. Wei, T. Hao, and Z. Zhou, *Polym. J*. **49**, 309 (2017).

[3]S. Joly, G. Garnaud, R. Ollitrault, L. Bokobza, and J. E. Mark, *Chem. Mater*. **14**, 4202 (2002).

[4]Y. Hirata, H. Kondo, and Y. Ozawa, "Natural Rubber (NR) for the Tyre Industry," in *Chemistry, Manufacture, and Applications of Natural Rubber,* Elsevier, Amsterdam, 2014, pp. 325–352. doi:10.1533/9780857096913.2.325

[5]V. N. Khiêm and M. Itskov, *J. Mech. Phys. Solids* **116**, 350 (2018).

[6]K. Cornish, "Biosynthesis of Natural Rubber (NR) in Different Rubber-Producing Species," in *Chemistry, Manufacture and Applications of Natural Rubber,* Elsevier, Amsterdam, 2014. doi:10.1533/9780857096913.1.3

[7]H. Mooibroek and K. Cornish, *Appl. Microbiol. Biotechnol*. **53**, 355 (2000).

[8]International Rubber Study Group, "Statistical Summary of World Rubber Situation," *Rubber Stat. Bull*. **1** (2017).

[9]Association of Rubber Producing Countries, "ANRPC Releases Natural Rubber Trends & Statistics July 2017," July 10, 2017, http://www.anrpc.org/html/news-secretariat-details.aspx?ID=9&PID=39&NID=1208. Accessed date August 5, 2017.

[10]M. Moore, "NR Prices Remain Low Despite Supply Shortfall," August 7, 2017, https://www.rubbernews.com/article/20170807/NEWS/170809947/nr-prices-remain-low-despite-supply-shortfall. Accessed date January 10, 2019.

[11]Association of Rubber Producing Countries, "ANRPC Releases Natural Rubber Trends and Statistics December 2017," January 18, 2018, http://www.anrpc.org/html/news-secretariat-details.aspx?ID=9&PID=39&NID=1702. Accessed date August 10, 2018.

[12]European Commission, "Communication from the Commission to the European Parliament, the Council, the European Economic and Social Committee and the Committee of the Regions on the 2017 list of Critical Raw Materials for the EU 1–8," September 13, 2017, http://eur-lex.europa.eu/legal-content/EN/TXT/PDF/?uri=CELEX:52017DC0490&from=EN. Accessed date November 28, 2017.

[13]N. N. Bich, "Natural Rubber Trends & Statistics," May 2018, News From Secretariat, http://www.anrpc.org/html/news-secretariat-details.aspx?ID=9&PID=39&NID=1923. Accessed date July 13, 2018.

[14]Ikeda, Y., P. Junkong, T. Ohashi, T. Phakkeeree, Y. Sakaki, A. Tohsan, S. Kohjiya, and K. Cornish, *RSC Adv*. **6**, 95601 (2016).

[15]C. S. Barrera, A. B. O. Soboyejo, and K. Cornish, RUBBER CHEM. TECHNOL. **91**, 79 (2017). doi:10.5254/rct.82.83716

[16]C. S. Barrera and K. Cornish, *J. Polym. Environ*. **23**, 437 (2015).

[17]C. S. Barrera and K. Cornish, *Ind. Crops Prod*. **107**, 217 (2017).

[18]C. S. Barrera and K. Cornish, *Ind. Crops Prod*. **86**, 132 (2016).

[19]D. Rasutis, K. Soratana, C. McMahan, and A. E. A. Landis, *Ind. Crops Prod*. **70**, 383 (2015).

[20]C. McMahan, D. Kostyal, D. Lhamo, and K. Cornish, *J. Appl. Polym. Sci*. **132**, 1 (2015).

[21]K. Cornish, *Technol. Innov*. **18**, 244 (2017).

[22]D. A. Ramirez-Cadavid, K. Cornish, and F. C. Michel, *Ind. Crops Prod*. **107**, 624 (2017). doi:10.1016/j.indcrop.2017.05.043

[23]B. Iaffaldano, Y. Zhang, and K. Cornish, *Ind. Crops Prod*. **89**, 356 (2016).

[24]European Commission, "Home-Grown Rubber to Keep Tyres Turning," European Commission 1, April 13, 2015, https://ec.europa.eu/programmes/horizon2020/en/news/home-grown-rubber-keep-tyres-turning. Accessed date November 28, 2017.

[25]D. J. Siler, K. Cornish, and R. G. Hamilton, *J. Allergy Clin. Immunol*. **98**, 895 (1996).

[26]R. G. Hamilton and K. Cornish, *Ind. Crops Prod*. **31**, 197 (2010).

[27]P. Junkong, K. Cornish, and Y. Ikeda, *RSC Adv*. **7**, 50739 (2017).

[28]F. C. Lockwood and J. E. Van Niekerk, *Combust. Flame* **103**, 76 (1995).

[29]A. S. Hashim, B. Azahari, Y. Ikeda, and S. Kohjiya, RUBBER CHEM. TECHNOL. **71**, 289 (1998).

[30]N. Rattanasom, T. Saowapark, and C. Deeprasertkul, *Polym. Test*. **26**, 369 (2007).

[31]J. Li, A. I. Isayev, X. Ren, and M. D. Soucek, RUBBER CHEM. TECHNOL. **89**, 608 (2016).

[32]J. Schlomach and M. Kind, *J. Colloid Interface Sci*. **277**, 316 (2004).

[33]R. A. Livingston, *Atmos. Environ*. **146**, 332 (2016).

[34]P. J. Martin, P. Brown, A. V. Chapman, and S. Cook, RUBBER CHEM. TECHNOL. **88**, 390 (2015).

[35]M. O. Amdur, *Environ. Health Perspect*. **81**, 109–13 (1989).

[36]S. S. Sarkawi, W. K. Dierkes, and J. W. M. Noordermeer, *Eur. Polym. J*. **49**, 3199 (2013).

[37]P. Yu, H. He, Y. Jia, S. Tian, J. Chen, D. Jia, and Y. Luo, *Polym. Test*. **54**, 176 (2016).

[38]C. S. Barrera and K. Cornish, "Waste-Derived Reinforcing Fillers in Guayule and Hevea Natural Rubber," presented at the 190th Technical Meeting of the Rubber Division, ACS, Pittsburgh, October 10–13, 2016.

[39]U.S. Department of Agriculture, *Chickens and Eggs,* National Agricultural Statistics Service, Washington, D.C., 2017.

[40]W. T. Tsai, J. M. Yang, C. W. Lai, Y. H. Cheng, C. C. Lin, and C. W. Yeh, *Bioresour. Technol*. **97**, 488 (2006).

[41]K. A. Iyer and J. M. Torkelson, *Compos. Sci. Technol*. **102**, 152 (2014).

[42]J. Carvalho, J. Araujo, and F. Castro, *Waste Biomass Valorization* **2**, 157 (2011).

[43]Z. Mičicová, M. Pajtašová, S. Domčeková, D. Ondrušová, L. Ranik, and T. Liptáková, *Procedia Eng*. **136**, 239 (2016).

[44]K. Cornish, U.S. Patent 5,580,942 (to U.S. Department of Agriculture) February 10, 1998.

[45]ASTM Standard D3182-16, "Standard Practice for Rubber—Materials, Equipment, and Procedures for Mixing Standard Compounds and Preparing Standard Vulcanized Sheets," *Annual Book of ASTM Standards* (2017). doi:10.1520/D3182-16

[46]ASTM Standard D6814-02, "Standard Test Method for Determination of Percent Devulcanization of Crumb Rubber Based on Crosslink Density," *Annual Book of ASTM Standards* **02**, 2013–2015 (2014).

[47]P. J. Flory and J. Rehner, *J. Chem. Phys*. **11**, 512 (1943).

[48]P. P. Kulkarni and C. T. Jafvert, *Environ. Sci. Technol*. **42**, 845 (2008).

[49]ASTM Standard D412-15a. "Standard Test Methods for Vulcanized Rubber and Thermoplastic Elastomers—Tension," *Annual Book of ASTM Standards* **i**, 1–14 (2012).

[50]ASTM Standard D2240-15, "Standard Test Method for Rubber Property—Durometer Hardness," *Annual Book ASTM Standards* **1–7** (2012). doi:10.1520/D1415-06R12.2

[51]J. R. Benjamin and C. A. Cornell, *Probability, Statistics, and Decision for Civil Engineers,* Courier Corporation, North Chelmsford, MA, 2014.

[52]A. H.-S. Ang and W. S. Tang, *Probability Concepts in Engineering: Emphasis on Applications in Civil and Environmental Engineering*, John Wiley & Sons, New York, 2006.

[53]O. D. Wangensteen, D. Wilson, and H. Rahn, *Respir. Physiol*. **11**, 16 (1970).

[54]K. C. Baranwal and H. L. Stephens, *Basic Elastomer Technology*, Rubber Division, American Chemical Society, Akron, OH, 2001.

[55]M. Wang, RUBBER CHEM. TECHNOL. **71**, 520 (1998).

[56]M.-J. Wang, S. Wolff, and J.-B. Donnet, RUBBER CHEM. TECHNOL. **64**, 559 (1991).

[57]A. Ansarifar, R. Nijhawan, T. Nanapoolsin, and M. Song, RUBBER CHEM. TECHNOL. **76**, 1290 (2003).

[58]M. Yrieix and J.-C. Majesté, *Eur. Polym. J*. **94**, 299 (2017).

[59]M. Castellano, L. Conzatti, G. Costa, L. Falqui, A. Turturro, B. Valenti, and F. Negroni, *Polymer (Guildf)*. **46**, 695 (2005).

[60]T. Fukuda, S. Fujii, Y. Nakamura, and M. Sasaki, *J. Appl. Polym. Sci*. **130**, 322 (2013).

[61]S. Wolff, RUBBER CHEM. TECHNOL. **55**, 967 (1982).

[62]S. M. A. Monadjemi, C. M. Mcmahan, and K. Cornish, *J. Res. Updates Polym. Sci*. **5**, 87 (2016).

[63]A. Ansarifar, N. Ibrahim, and M. Bennett, RUBBER CHEM. TECHNOL. **78**, 793–805 (2005).

[64]P. M. Visakh, S. Thomas, K. Oksman, and A. P. Mathew, *Compos. Part A Appl. Sci. Manuf.* **43**, 735–741 (2012).

[65]PPG Industries, "Hi-Sil™ 190G and 190G-M," July 8, 2008, http://www.ppgsilica.com/getmedia/8de74009-d609-4f6c-b44e-6ea2e56f8b23/HiSil190Gand190GMBrochure.pdf.aspx. Accessed date January 11, 2019.

[66]U.S. Energy Information Administration, "Electricity Explained—Electricity in the United States," April 20, 2018, https://www.eia.gov/energyexplained/index.cfm?page=electricity_in_the_united_states. Accessed date August 6, 2017.

[67]American Egg Board, "About the U.S. Egg Industry," *Industry Overview* 1 (2017), http://www.aeb.org/farmers-and-marketers/industry-overview. Accessed date November 27, 2017.

[68]Jinzhou Hancheng Chemicals Co., Carbon Black N234 Product on Alibaba.com, https://www.alibaba.com/product-detail/Virgin-type-pyrolysis-Carbon-black-N234_60183857095.html?spm=a2700.7724838.2017115.46.433fd256a8jzSi. Accessed date October 30, 2017.

[69]Weifang Longstar Economy and Trading Co., Precipitated Silica Product, *Alibaba.com* (2017), https://www.alibaba.com/product-detail/precipitated-silica-white-carbon-black-used_60220460375.html?spm=a2700.7724857.main07.12.396aa4c1Mx0EMn&s=p. Accessed date: October 30, 2017.

[70]A. S. M. Bashir and Y. Manusamy, *J. Eng. Res. Technol.* **2**, 56 (2015).

[71]ASTM Standard D2000-12, "Standard Classification System for Rubber Products in Automotive Applications," *Annual Book of ASTM Standards* **1** (2017). doi:10.1520/D2000-12.2

[72]ASTM Standard D4388-13, "Standard Specification for Nonmetallic Semi-Conducting and Electrically Insulating Rubber Tapes," *Annual Book of ASTM Standards* **1–3** (2013). doi:10.1520/D4388-13.2

[73]ASTM Standard D1330-04, "Standard Specification for Rubber Sheet Gaskets," *Annual Book of ASTM Standards* **04**, 1–3 (2015).

[74]K. Cornish, J. L. Brichta, P. Yu, D. Wood, M. Mcglothlin, and J. A. Martin, *Ind. Crop.* 1–5 (2002).

[*Received September 2018, Accepted November 2018*]